

Sustainable styrene-butadiene composites with sisal fiber and rubber waste from footwear

Alexandre Oka Thomaz Cordeiro¹ , Marcelo Eduardo da Silva¹  and Cristiane Reis Martins^{1*} 

¹*Laboratório de Engenharia e Controle Ambiental, Departamento de Engenharia Química, Instituto de Ciências Ambientais, Químicas e Farmacêuticas, Universidade Federal de São Paulo, Diadema, São Paulo, SP, Brasil*

*cr.martins@unifesp.br

Abstract

This study examines the impact of three surface treatment methods on sisal fibers used as reinforcement in styrene-butadiene rubber (SBR) composites: washing with water, alkaline treatment (mercerization), and silanization, with each composite containing 5 wt% of fibers. The preparation process involved using an internal mixer and rubber mixing mill to shape the composites, followed by vulcanization in an automated system press. The effectiveness of the treatments was evaluated using scanning electron microscopy, along with tensile tests, rheometer analysis, and measurements of hardness and density. The treatments enhanced fiber modification by increasing surface roughness through the grafting of silanol groups, thereby improving their interaction with the elastomeric matrix. Notably, composites reinforced with silanized fibers exhibited the highest performance and interaction among the various treatment methods, showing a higher modulus at 100%. Alkaline and silanization treatments reduced vulcanization time. Sisal fibers combined with SBR waste can promote sustainability in the footwear industry.

Keywords: *fiber surface treatment, sisal fiber, styrene-butadiene rubber, footwear industry, composites.*

Data Availability: Research data is available upon request from the corresponding author.

How to cite: Cordeiro, A. O. T., Silva, M. E., & Martins, C. R. (2025). Sustainable styrene-butadiene composites with sisal fiber and rubber waste from footwear. *Polímeros: Ciência e Tecnologia*, 35(3), e20250035. <https://doi.org/10.1590/0104-1428.20250004>

1. Introduction

Growing concerns about production waste and its environmental impact have led to changes in the footwear industry. Implementing a circular economy and finding new uses for the waste generated by the industry is an option to reduce environmental impacts and promote sustainability. Another solution to promote sustainability is using materials from renewable and/or biodegradable sources, such as plant fibers^[1-5].

The circular economy is a concept that focuses on delivering positive benefits for society, aiming to reduce waste in the production chain and promote the reuse of resources. Currently, most of the waste from the footwear industry is discarded, causing a negative environmental impact on the industry. As a solution, incorporating waste into new composites and products can be a way to add value to the material and promote sustainability^[1,3,6]. In addition to the automotive sector, the footwear industry, which uses SBR extensively, is one of the primary producers of styrene-butadiene rubber (SBR) waste^[7,8]. Concern about environmental pollution and the waste of raw materials with suitable properties and high added value motivates the reuse of this rubber^[9-12]. One method of recycling this residue is to mill it into a fine powder, making it easier to flow and mix with virgin resin to produce new

formulations. In this way, it can be used as a consumable in a new process^[7,8,13,14].

A further method to enhance sustainability in the footwear industry involves a new category of materials for footwear production: biodegradable materials and renewable sources, including vegetable fibers such as sisal, cotton, flax, bamboo, coconut, hemp, cork, and soy^[1,4,15]. Vegetal fibers offer several advantages, including low density, low cost, high availability, biodegradability, ease of acquisition and handling, and ecological benefits from their renewable sources^[16-18]. Sisal is one of the most utilized vegetable fibers in elastomeric matrix composites. It stands out beyond its ecological aspect as its cultivation plays a vital role in enhancing agriculture in the northeast semiarid regions of Brazil^[16,19-25].

However, fibers are incompatible with most matrices because of their composition and hydrophilic nature. In polymer composites, high moisture fibers can impact their final properties, and the hydrophilic nature of the fibers makes it very difficult to disperse within a hydrophobic rubber matrix^[17,26-28]. Several surface modification methods are used, including both physical and chemical treatments, and coupling agents are used to improve interfacial bonding between fibers and matrix^[28-31]. Alkaline treatments increase possible reaction sites and surface roughness. In contrast,

silane treatments promote a stable surface on the fiber and create hydrogen bonds between the silane molecule and the hydrogens of the polymer matrix. Both treatment methods are commonly used for vegetable fibers reinforcing thermoplastic, thermoset, and rubber composites^[18,26,27,32]. There are few studies on the effects of incorporating vegetal fibers into elastomeric matrices compared to other polymer matrices.

To promote sustainability, this study aims to develop a composite formulation for footwear applications by reusing SBR residues from the footwear industry and incorporating sisal fibers treated with various surface methods. The work involves characterizing the composite's mechanical and morphological properties, evaluating the impact of sisal fiber incorporation on these properties, and assessing the technical feasibility of utilizing the material in sandal production for the footwear industry.

2. Materials and Methods

2.1 Materials

In this study, the following materials were used: sodium hydroxide (NaOH) P.A. (Labsynth); Silquest A-178 methacryloxypropyltrimethoxysilane (Momentive); sisal fibers (refugo type), supplied by Hamilton Rios (Conceição do Coité, BA, Brazil); and two grades of random poly(styrene-butadiene) (SBR) elastomer copolymers, referred to as SBR A and SBR B, with approximate styrene contents of 23.5% and 48%, respectively. The rubber formulation in this work resembles a compound derived from expanded vulcanized SBR waste generated by the footwear industry. Alpargatas SA kindly supplied all ingredients.

2.2 Sisal fiber treatments

Sisal fibers were cut to a precise length of 6 mm using a guillotine paper cutter. The fibers were then ground in a knife mill (Tecnal) and effectively sieved through a Tyler 16 sieve with a 1 mm opening. The following superficial treatments were evaluated to increase the interfacial interaction between sisal fibers and the elastomeric matrix. Washed sisal fibers (WSF) were washed in deionized water under agitation for 1 h at 80 °C and then dried in an air circulation oven at 60 °C for 12 h^[22]. Mercerized sisal fibers (MSF) were treated with agitation in a 5% NaOH solution at room temperature (21 °C) for 3 h, then washed until neutralized pH (~7) and dried in an air circulation oven at 60 °C for 12 h^[22]. Silanized sisal fibers (SSF) were washed in deionized water under agitation for 1 h at 80 °C and dried in an air circulation oven at 60 °C for 12 h. A 0.3% solution of γ -methacryloxypropyltrimethoxysilane in alcohol (60% ethanol in water) was prepared. Fibers were submerged in agitation with the silane solution at 1:3 (silane to fiber) for 90 min at room temperature. Afterward, fibers were dried in an air circulation oven at 70 °C for 24 h until constant weight was achieved^[31].

2.3 Rubber compounding process and composites preparation

Rubber compounds were prepared by blending varying SBR A and SBR B concentrations, incorporating SBR waste from the footwear industry. The mixing process was

performed using a Banbury internal mixer BT (Luxor) located at Flexlab (Santo André, São Paulo, Brazil) under the following conditions with 60 rpm and a piston pressure of 5 kgf/cm².

Figure 1 illustrates the methodology adopted for treating sisal fibers and preparing SBR/Sisal fiber (SF) composites. The formulations used in preparing the rubber and composite are detailed in Table 1. A preliminary study was conducted to ensure that the developed formulation would resemble the properties of rubber waste provided by the footwear industry. Figure 1a shows the sisal fibers following various surface treatments, while Figure 1b presents the two types of SBR elastomers utilized. In the first mixing stage, the SBR elastomers were added to a Banbury mixer and masticated for one minute. Subsequently, all other ingredients, excluding sulfur and sisal fibers, were incorporated and mixed for three minutes. In the second stage, sulfur was added and mixed for one minute, achieving a total mixing time of five minutes. The compound was then transferred to a two-roll mill (MBL, Luxor) for further homogenization for approximately 10 minutes before being sheeted out, followed by a 24 hour resting period at room temperature (Figure 1c). The SBR/SF composites were prepared on the same two-roll mill by incorporating 8.8 phr of treated sisal fibers into the SBR60/40 blend (Figure 1c). A portion of the material, both with and without sisal fibers, was used to determine optimal curing conditions. The remaining material was vulcanized in a hydraulic press at 160 °C for 15 minutes (Figure 1e). Figure 1f displays a final product manufactured from the SBR/SF composite.

2.4 Fiber characterization

For morphological analysis, the fibers' surfaces were examined using scanning electron microscopy (SEM) 6610 L20 (JEOL JSM) at an acceleration voltage of 5 kV. For all treatments, the surfaces were coated with gold.

Table 1. Formulations in phr in SBR rubber and composites (SBRc) preparation.

Materials	Formulations (phr)			
	SBR50/50	SBR60/40	SBR70/30	SBR60/40c
Styrene-butadiene rubber (SBR-A)	50	40	30	40
Styrene-butadiene rubber (SBR-B)	50	60	70	60
SBR waste	16.66	16.66	16.66	16.66
Silica	16.66	16.66	16.66	16.66
Kaolin	16.66	16.66	16.66	16.66
ZnO	3	3	3	3
PEG ^c	3	3	3	3
Sulfur	2	2	2	2
Stearic acid	1	1	1	1
Antioxidant ^b	1	1	1	1
MBT ^a	1.5	1.5	1.5	1.5
Mineral Oil	10	10	10	10
Azodicarbonamide	5	5	5	5
Sisal fibers (SF)	0	0	0	8.86

^aMBT = Mercaptobenzothiazole; ^bAntioxidant = Styrenated Phenol;

^cPEG = Polyethylene Glycol.

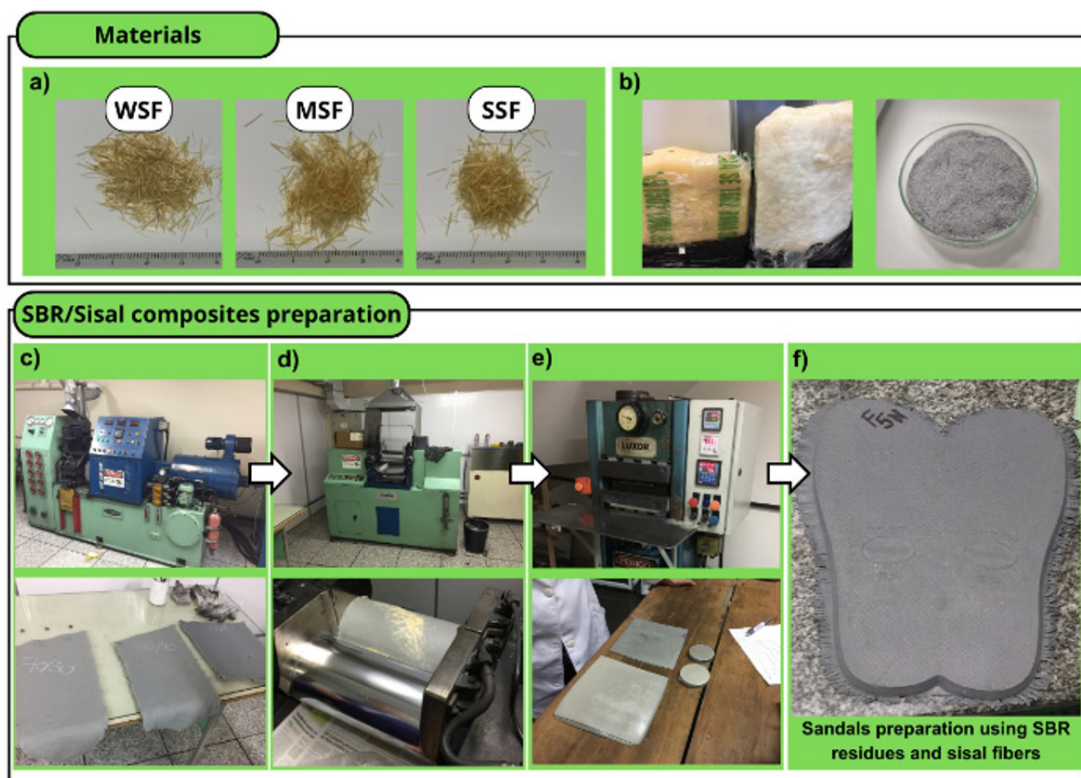


Figure 1. Schematic diagram of the preparation process of SBR/SF composites: (a) sisal fiber with treatments, (b) SBR rubbers and waste, (c) Banbury internal mixer, (d) two-roll mill, (e) vulcanization process in a hydraulic press, (f) sandals produced by SBR/SF composite.

The Fourier Transform Infrared (FTIR) Spectrophotometer (IR Prestige, Shimadzu Corporation) was used to analyze the functional compounds in the sisal fibers subjected to various treatments. The FTIR scans were conducted in the wavenumber range of 4000 to 500 cm^{-1} , with a resolution of 4 cm^{-1} and a total of 128 scans. These measurements were performed in a controlled environment with regulated temperature and humidity, using transmittance mode based on the wavelength.

The thermogravimetric (TGA) technique evaluated the sisal fibers' thermal behavior before and after treatment. The analysis was conducted on a DTG-60H (Shimadzu) located at NIPE from Unifesp, Campus Diadema, São Paulo. Tests were carried out under an N_2 atmosphere with a gas flow rate of 50 mL/min , a heating rate of 10 °C/min , and a temperature range from 30 to 600 °C .

2.5 Rubber compounds and SBR/SF composites characterization

Rheological analysis was used to understand the formulations' vulcanization behavior. Samples were analyzed using a motorless cure rheometer MDR 2000 (Alpha Technologies) located at Flexlab. The tests were carried out at 160 °C for 30 minutes, according to ASTM D5289-19a. Disk format samples of about 7 g with an approximate volume of 5 cm^3 were used.

Hardness tests were measured with a Shore A durometer TEC-017 (X.F. Instruments) using five samples for each

specimen according to NBR 14454/07. The density was obtained by Archimedes' method according to NBR 1739/10.

Stress-strain tests were conducted using a universal testing machine, Tensometer 2000 (Monsanto), located at Flexlab, following the ASTM D412-06A standard. The samples used were of type C shape (dimensions). The cross-head feed rate was set to 500 mm/min , and a load cell with a capacity of 1.0 kN was employed. Five samples of each formulation were used.

The mechanical properties results were statistically evaluated using Analysis of Variance (ANOVA), applying Tukey's test at a 5% significance level, with the aid of Minitab® 16.0 software.

The microscopy images were obtained using a scanning electron microscope (SEM) 6610 L20 (JEOL JSM), with a gold coating applied to the samples fractured cryogenically.

3. Results and Discussions

3.1 Sisal fibers characterization

Figure 2 shows the SEM micrograph of the surface of sisal fibers with and without treatment. Figure 2a shows that untreated fibers have a surface with microfibril cellulose structures that are barely exposed and covered by the sedimentary materials that make up their surface, with no definition of the parenchyma regions of the sisal fiber. This is different from what was observed in other works^[19,23,33], which may be related to the fact that the fibers are of the refugo type and have lower quality^[34].

Compared to other types of sisal fiber supplied by the company, in addition to the fact that the fibers may present variations in their composition according to their origin and position on the leaf from which they were obtained^[23]. The SEM micrographs of the fibers after washing with water (WSF) are shown in Figure 2b. The SEM micrographs of the fibers after the alkaline treatment (MSF) are shown in Figure 2c, and silanized sisal fibers (SSF) are shown in Figure 2d. By comparing the micrographs in Figures 2a and 2b between the untreated fibers and the washed fibers, partial removal of the materials that cover the surface can be observed, as well as the appearance of well-defined regions of the parenchyma on the surface of the fiber. Unlike the results obtained in the literature, where washing the fiber did not generate notable changes in its appearance^[33], this treatment proved effective for waste-type fibers.

In the alkaline treatment, the extraction of hemicellulose, lignin, as well as waxes, greases, and oils that make up the fiber, is observed, thus creating a more exposed surface with a smaller number of sedimentary materials and greater surface roughness that can lead to more significant mechanical interaction^[32]. Despite going through a washing step (Figure 2d), the silanized fibers present a different surface appearance than the only washed fibers. A smoother surface is observed without well-defined cell structures, which may be associated with eliminating substances that directly influence hydrophilicity, such as pectin, lignin,

and amorphous wax in fiber cuticles, through coupling agent treatments^[19].

FTIR analysis is a valuable technique for analyzing the structure of fibers and identifying changes that occur due to different treatments. This study used the FTIR spectrum to compare the untreated fibers with those treated with WSF, MSF, and SSF. The results for SF with and without treatment are shown in Figure 3. Fibers are known to consist mainly of cellulose, lignin, and hemicellulose. When fibers undergo alkaline treatment, a loss of mass occurs, which is attributed to the dissolution of hemicellulose. This is confirmed by the disappearance of the carbonyl group band at 1730 cm^{-1} in the FTIR curve of the alkaline-treated fibers compared to the untreated fibers^[31]. In the case of silanization treatment, the silane bonds with hydroxyl groups of the fiber surface^[35]. The introduction of an amine group (NH_2) is expected. A band can identify this at 3200 cm^{-1} in the FTIR spectrum. Additionally, the silanization treatment leads to higher intensity absorbance related to the Si-O and Si-O-Si groups, which can be observed at 1285 , 1075 , and 1018 cm^{-1} , respectively^[36-38]. The low silane concentration and weak interaction with fiber components may limit the detection of silanization effects in the FTIR spectra. The Si-O-C bond is difficult to identify due to strong cellulose absorption between $1000\text{--}1200\text{ cm}^{-1}$ ^[39]. However, the reduced intensity of the 1023 cm^{-1} peak, where Si-O-C and C-O bands overlap after treatment, suggests the formation of Si-O-C bonds.

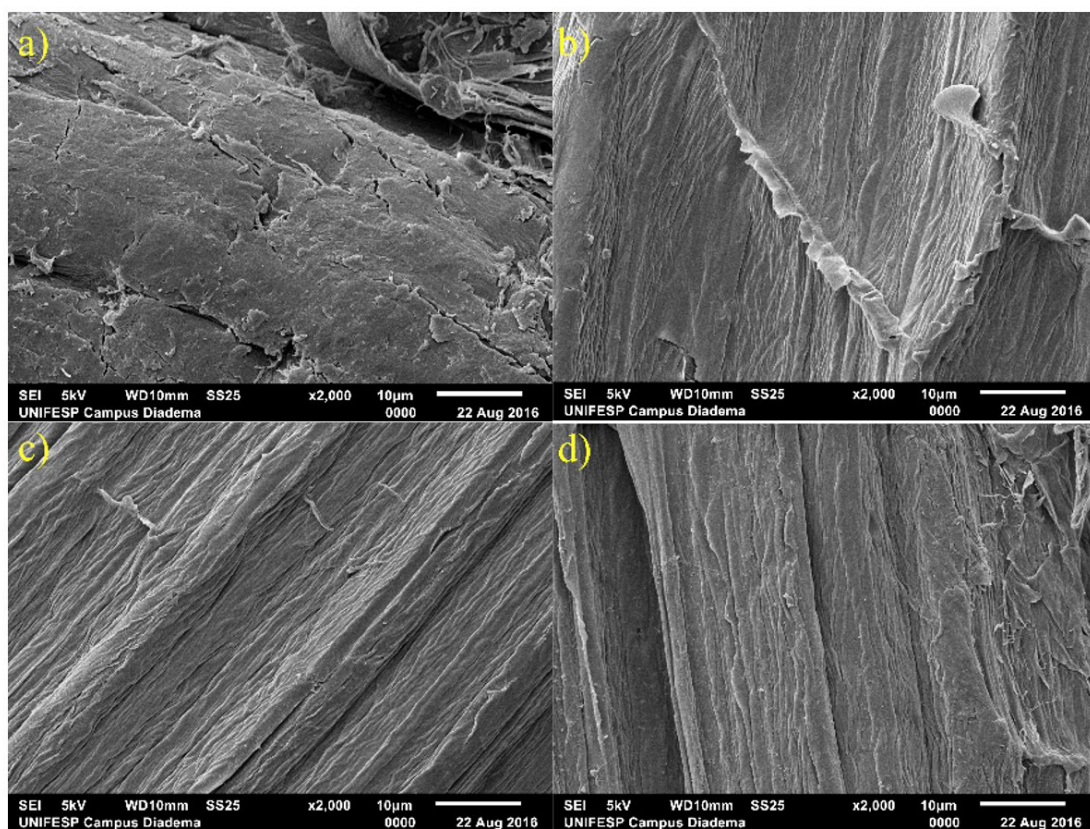


Figure 2. SEM micrographs of sisal fibers with and without treatment. (a) natural sisal fibers; (b) washed sisal fibers; (c) mercerized sisal fibers; (d) silanized sisal fibers at 200x magnification.

The thermal characteristics of untreated and variously treated sisal fibers have been examined. The TGA curves are shown in Figure 4a, and the DTG curves are shown in Figure 4b. The thermal analysis results show three main stages of mass loss of the fiber during its degradation. The first stage occurred at up to about 100 °C, which may be related to the loss of water associated with the moisture present in the fibers and volatile compounds such as waxes, fats, and oils. The second stage occurred between 200 and 360 °C. This mass loss stage is linked to the degradation process of hemicellulose and cellulose present in the fiber. The third stage commenced at 400 °C. The degradation of lignin occurs more slowly and at higher temperatures than that of hemicellulose and cellulose. Although they all undergo drying stages, the complete removal of water is hindered due to the hydrophilic nature of the fibers. SF exhibits thermal stability between a 100 to 190 °C, while treated fibers withstand up to 200 to 220 °C. The increase in the thermal resistance of the fibers after treatment may be associated with the partial removal of hemicellulose, lignin, waxes and fats. For WSF, where the removal of these materials is more extensive, better thermal stability is observed^[25,40,41].

3.2 SBR characterization

By varying the amount of SBR B and SBR A in the rubber formulation (1) 50/50% (SBR50/50), (2) 60/40% (SBR60/40), and 70/30% (SBR70/30) of SBR B and SBR A, respectively, we obtained pure rubber blankets. The influence of the two different types of SBR on the sulfur vulcanization of the prepared rubber compounds was evaluated based on selected parameters of the vulcanization characteristics from the rheological records of their vulcanization curves. The curing parameters were assessed: minimum torque (ML), maximum torque (MH), the difference between MH and ML (ΔM) (Equation 1), scorch time (t_{s1}), optimum cure time (t_{90}), and cure rate index (CRI) (Equation 2). The values of the basic parameters of vulcanization characteristics of individual rubber compounds containing SBR are shown in Table 2.

$$\Delta M = M_H - M_L \quad (1)$$

$$CRI = \frac{100}{t_{90} - t_{s1}} \quad (2)$$

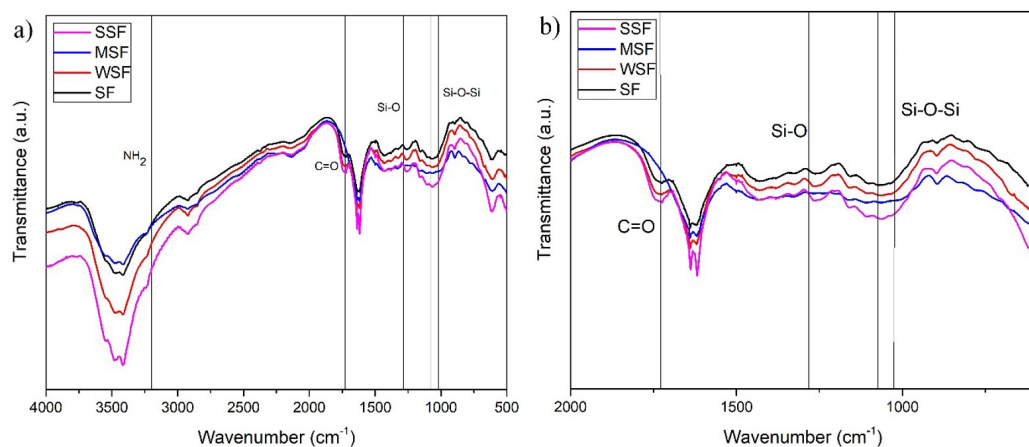


Figure 3. Impact of different surface treatments on FTIR spectra of sisal fibers (SF), washed sisal fibers (WSF), mercerized sisal fibers (MSF), and silanized sisal fibers (SSF). FTIR (a) zoom in the range of 4000-500 cm^{-1} and (b) of 2000-600 cm^{-1} .

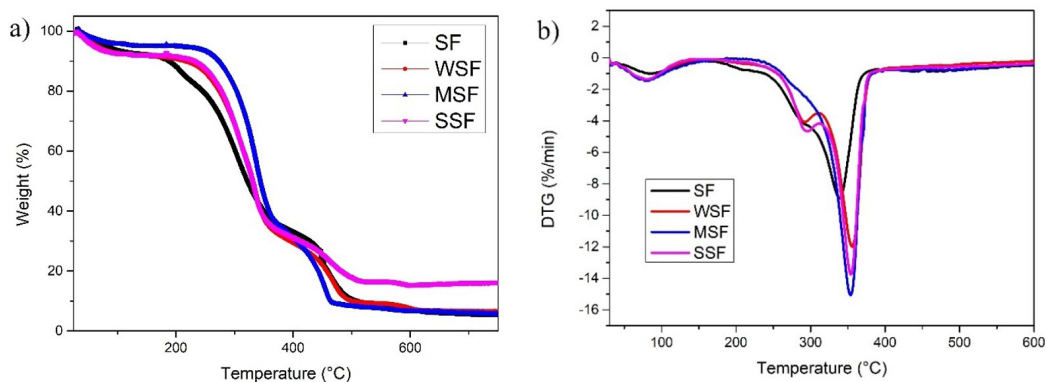


Figure 4. The (a) TGA thermograms and (b) DTG thermograms of sisal fibers (SF), washed sisal fibers (WSF), mercerized sisal fibers (MSF), and silanized sisal fibers (SSF).

Curing parameters change notably with blend ratios. ML is the rigidity and viscosity of an unvulcanized elastomer and an indicator of its processability. As the SBR B increases in ratio, a slight increase in ML is observed. MH directly relates to the compound's modulus and measures the material's stiffness. When the SBR B content increases, a lower MH is observed. This is due to increased styrene content in the compound, thus reducing MH. ΔM is an indicator of the cross-link density of the blends^[42]. As the content of SBR B increases, the compound contains more styrene and less butadiene, resulting in fewer active sites available for the sulfur vulcanization process. This decreases the cross-link density and lengthens the time required for the material to vulcanize, as evidenced by the higher ts1 and t90 numbers and a lower observed CRI value.

Table 3 presents the results of the mechanical tests of the rubber formulations. There was no significant change regarding the mechanical properties of the SBR rubber compound, such as tensile strength, elongation at break, and modulus. The density increases with the ratio of styrene in the rubber compound. A slight increase in hardness is seen with the SBR60/40 formulation. We believe the rubber expansion causes the hardness to increase as the styrene ratio rises.

Figure 5 shows the micrographs obtained from the cryo-fractured surface of the rubber formulation SBR60/40. By analyzing the surface of these rubbers, the presence of many pores (closed cells) well-distributed throughout the matrix is observed. This characteristic is guaranteed by the blowing agent content in the rubber formulation due to the amount of gas produced from the thermal decomposition of azodicarbonamide^[43].

3.3 SBR/SF composites characterization

The SBR60/40 formulation was designed as the standard formulation for evaluating various fiber treatments. Due to its properties and that most closely resembles the composition of SBR waste used from the footwear industry. The values of the basic parameters of vulcanization characteristics of SBR composites containing SF are shown in Table 4.

Table 2. Rheological characteristics of SBR rubber compounds at different ratios.

	SBR50/50	SBR60/40	SBR70/30
ML (dN.m)	0.92	0.92	0.94
MH (dN.m)	9.77	9.3	8.32
ΔM (dN.m)	8.85	8.38	7.38
ts1 (min)	2.84	2.5	2.99
t90 (min)	13.19	15.51	17.03
CRI (min ⁻¹)	9.66	7.69	7.12

ML: minimum torque; MH: maximum torque; ΔM : difference between MH and ML; ts1: scorch time; t90: optimum cure time; CRI: cure rate index.

Table 3. Mechanical and physical properties of SBR rubber compound.

	SBR50/50	SBR60/40	SBR70/30
Tensile Strength (MPa)	6.21±0.20	6.46±0.43	6.00±0.15
Elongation at break (%)	448.38±9.67	445.94±21.86	466.24±6.50
M100 (MPa)	1.30±0.05	1.44±0.01	1.45±0.02
M200 (MPa)	2.20±0.08	2.44±0.03	2.40±0.03
M300 (MPa)	3.49±0.13	3.82±0.05	3.61±0.06
Hardness (Shore A)	40.17±2.15	44.17±1.63	38.67±3.47
Density (g/cm ³)	0.74±0.02	0.85±0.10	0.90±0.05

Table 4. Rheological characteristics of SBR/Sisal fibers composites.

	SBR60/40	SBR60/40W	SBR60/40M	SBR60/40S
ML (dN.m)	0.92	1.13	1.09	1.3
MH (dN.m)	9.3	10.89	10.51	10.89
ΔM (dN.m)	8.38	9.76	9.42	9.59
ts1 (min)	2.5	2.33	2.37	2.03
t90 (min)	15.51	16.38	15.33	14.87
CRI (min ⁻¹)	7.69	7.12	7.72	7.79

ML: minimum torque; MH: maximum torque; ΔM : difference between MH and ML; ts1: scorch time; t90: optimum cure time; CRI: cure rate index.

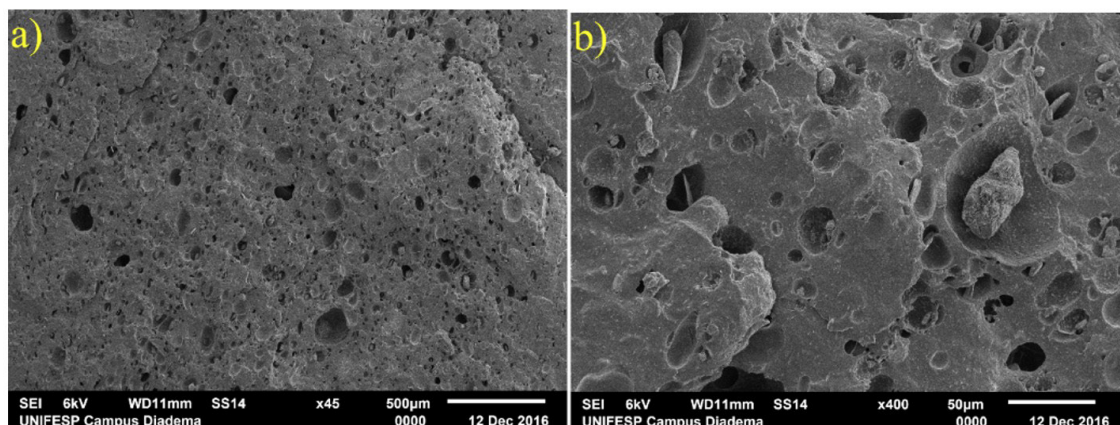


Figure 5. SEM micrographs of SBR60/40 surface at (a) 45x; (b) 400x magnification.

The measure results indicate the influence of sisal fibers on SBR rheological behavior. Fibers increased the rigidity and viscosity of the composite and its stiffness, as shown by more remarkable ML and MH values. This resulted in a higher reinforcement of the material in the composite, which can be attributed to improved interaction between fibers and the rubber matrix. Sisal fibers without treatment increased the vulcanization time, whereas silanized sisal fibers showed a lower vulcanization time. Curing chemical reactions occur in a base media, and adding a material that can increase the system's acidity may cause the initiation of curing chemical reactions to increase^[44,45]. These changes may be related to the acidity of the sisal fiber after each different treatment. The vulcanization process requires a significant amount of time and energy^[46]. Except for the sample that included WSF, there was a noticeable reduction in the time required for vulcanization when treated fibers were present. This reduction positively impacts the production time of the rubber artifact.

The micrographs in Figure 6 show the cryogenically fractured region of the SBR60/40 composites. The composites reinforced with fibers that were only washed (WSF, Figure 6a) and with silanization treatment (SSF, Figure 6c) exhibited better interaction with the matrix fiber compared to fibers treated with alkaline (MSF, Figure 6b). This was evident in the interface region between the matrix and fiber, where smaller distances between the materials indicated a better penetration of the elastomeric matrix on the fiber surface. Chemical treatments using agents such as silanes result in more significant fiber-matrix interaction by promoting a stable surface for adhesion. By creating hydrogen bonds between the silane molecule and the hydrogens in the polymer matrix, a stronger bond is achieved, leading to increased interaction between the fiber and the matrix^[31,32,36].

The micrographs of the fiber-reinforced composite with alkaline treatment (SBR60/40M) showed larger pores compared to other composites and low interaction of the fibers to the elastomeric matrix. This could be attributed to a significant amount of moisture in the fibers during processing. This hinders matrix interaction and results in large empty spaces and a smaller interface region than fibers that were only washed or silanized. Despite having a rougher surface due to

the treatment, the alkaline-treated fibers did not interact well with the matrix. This was evidenced during sample processing, where the material exhibited a high number of bubbles on its external surface compared to untreated composites, which may be attributed to the increased moisture content in the fibers treated with alkaline, causing exposure of hydroxyl groups in cellulose and resulting in a more hydrophilic material^[28]. In contrast to previous works which showed mechanical performance with mercerized and acetylated fibers^[22,47], it has been reported that alkaline treatment can increase moisture content in the fiber after treatment^[28,30] and adversely affect the expansion process of the material, leading to regions with high pore concentration.

Table 5 presents the mechanical results of the composites produced compared to the rubber formulations. The interaction between sisal fibers and the rubber matrix increases tensile strength. The filler particles and aggregates must be synchronized, well-dispersed, and wetted efficiently by the rubber matrix to increase the tensile strength. If not, inherent defects can act as stress concentration points and consequently decrease the tensile strength of the vulcanizates^[44].

Table 5. Mechanical and physical properties of SBR rubber compound and SBR/SF composites.

	SBR60/40	SBR60/40W	SBR60/40M	SBR60/40S
Tensile Strength (MPa)	6.46±0.43	5.18±0.28	3.25±0.10	5.93±0.17
Elongation at break (%)	445.94±21.86	443.28±24.88	358.00±76.60	435.32±8.95
M100 (MPa)	1.44±0.01	1.54±0.05	1.38±0.06	1.97±0.06
M200 (MPa)	2.44±0.03	2.30±0.05	2.03±0.24	2.74±0.05
M300 (MPa)	3.82±0.05	3.33±0.09	3.07±0.30	3.88±0.07
Hardness (Shore A)	44.17±1.63	56.67±1.53	46.00±2.00	62.33±3.06
Density (g/cm ³)	0.85±0.10	0.96±0.06	0.79±0.05	1.08±0.11

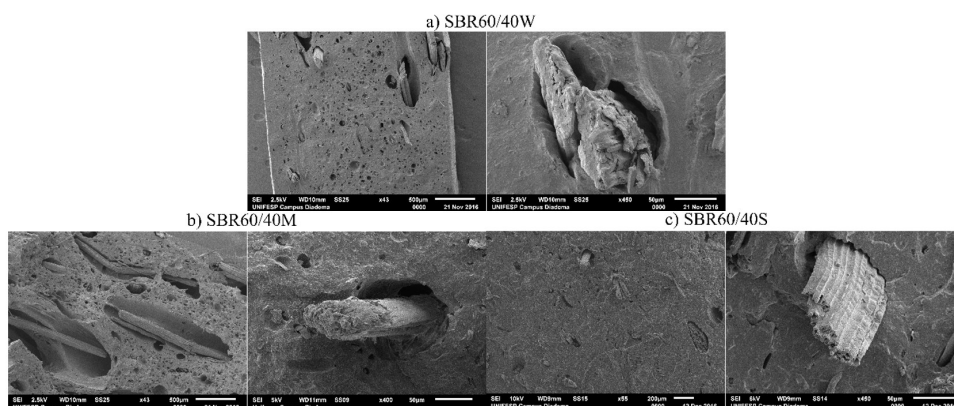


Figure 6. SEM micrographs of SBR and sisal fibers composites. (a) SBR60/40W at 43x and 450x magnification; (b) SBR60/40M at 43x and 400x magnification; (c) SBR60/40S at 55x and 450x magnification.

As observed in the SEM micrographs of the SBR/Sisal composites, the tensile results in Figure 7a for SSF showed no significant differences from the pure SBR compound. For WSF, a decrease in tensile results is observed. With only the partial removal of materials covering the surface of the sisal fiber through washing, it was not enough for the fibers to act as reinforcement in the composite. As observed in SEM micrographs, MSF exhibited interaction with the rubber matrix. Thus, lower tensile strength was obtained. For SSF, using silanes resulted in more significant fiber-matrix interaction than other treatments.

Composites incorporated only with MSF reduce the elongation at break, as shown in Table 5 and Figure 7b.

Incorporating poorly adhering fillers into a rubber matrix disrupts chain alignment. These results in weaker interfacial regions between the filler surface and the rubber matrix, as seen in SEM micrographs (Figure 6b). Fractures at lower elongation can occur due to cracks traveling quickly through weaker interfacial areas^[19,25,44,45,47].

Stresses were determined at different elongations to understand the evolution of deformation resistance of the SBR compound in the presence of SF upon loading. Figure 8 shows the M100, M200, and stress at 300% (M300) over different treated sisal fibers. Adding rigid and stiff particle fillers increases the composites' modulus by restricting the polymer molecules' movement.

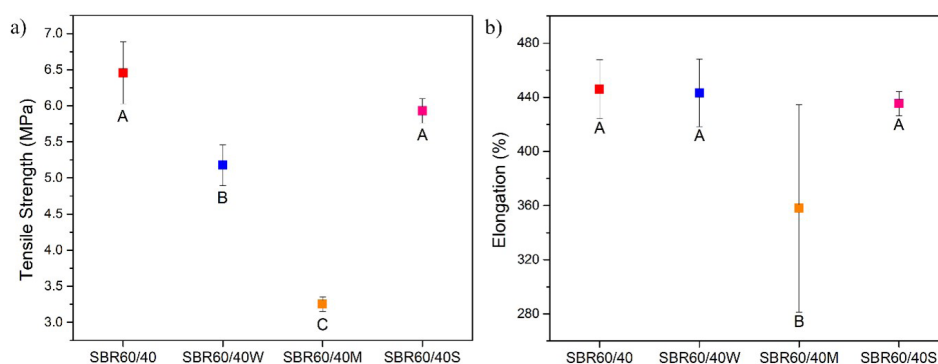


Figure 7. (a) Tensile strength and (b) elongation results of the studied SBR/Sisal fibers composites. The letters represent significant statistical analysis differences ($p < 0.05$; ANOVA followed by Tukey's test).

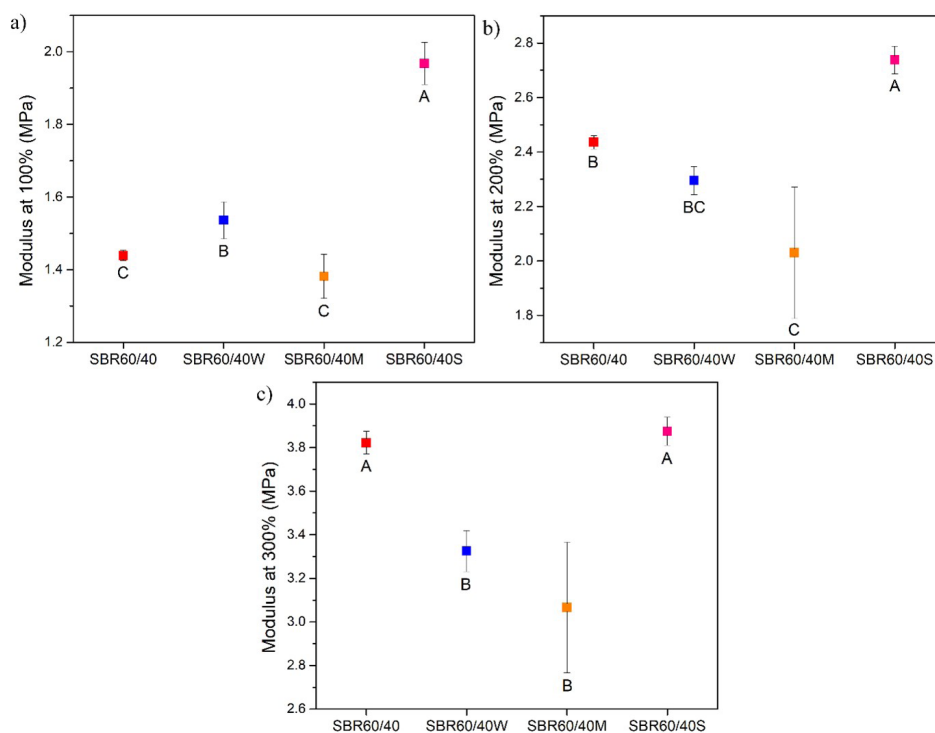


Figure 8. Modulus at (a) 100%, (b) 200%, and (c) 300% results of the studied SBR/Sisal fibers composites. The letters represent significant statistical analysis differences ($p < 0.05$; ANOVA followed by Tukey's test).

Modulus is influenced by surface reactivity, aggregation, particle size and shape, structure, and particle dispersion in rubber^[42,44]. This effect is only observed by SBR60/40S, in which the modulus was markedly increased compared to pure SBR and other SBR/Sisal composites. Also, it could be due to the increase in the cross-link density observed in the rheological tests in the presence of the signalized sisal fibers.

Understanding the influence of fibers on the hardness of the final material is essential for the footwear industry, as hardness directly affects the perceived comfort of footwear^[48]. The addition of sisal fibers increases the hardness of the composite by restricting the mobility of rubber chains, resulting in a more rigid material structure. Hardness is closely related to elastic modulus; therefore, an increase in hardness is expected, as cellulose particles have a higher modulus than the rubber matrix^[44,45]. In general, the density of vegetable fibers is lower compared to rubber. Depending on the volume of a fraction of the fibers, the composite's overall density may decrease when added to the rubber matrix. However, as observed in the SEM micrographs (Figure 6), the sisal fibers in the rubber matrix can influence the expansion process during the thermal degradation of the blowing agent azodicarbonamide. Composites containing SSF exhibited fewer pores than those with other treated fibers, which may be attributed to the increased material density. Previous studies on sisal and wood flour have reported that silane treatments can enhance hardness^[49,50]. Accordingly, the improved interfacial adhesion between the fiber and the rubber matrix, as evident in the SEM micrographs, likely facilitates more efficient stress transfer, contributing to increased hardness and elastic modulus in the SSF reinforced composites.

Regarding the mechanical properties of the composites, tensile strength, elongation at break, and modulus, the Tukey test revealed significant differences among all fiber-reinforced formulations, except for the SSF composite. Despite the known incompatibility between vegetal fibers and the SBR matrix, silanization treatment improved interfacial adhesion. This allowed the treated sisal fiber composites to achieve mechanical performance comparable to the reference while demonstrating a notably higher modulus at 100%.

4. Conclusions

A formulation of the SBR compound was successfully developed by efficiently utilizing and incorporating SBR waste. Formulation modifications determined by the content of two types of SBR significantly affect the compound's final properties. Lower styrene concentrations in the rubber result in a reduced vulcanization time.

After being incorporated into the SBR matrix, the silanization treatment was only applied to sisal fibers, resulting in better mechanical performance. Compared to the pure SBR compound, silanized sisal fiber composites displayed a greater modulus at 100 and 200%. The presence of the fibers also increases the composite's hardness.

This study underscores the considerable potential of sisal fibers in developing sustainable composites. Combining SBR waste from the footwear industry with this renewable material, which holds significant social and economic value, can pave the way for innovative and eco-friendly products.

These composites can meet industry demands and transform the sector through adjustments to the formulation and treatment of the fibers. Future research will aim to increase fiber concentration and optimize the composition to enhance their application in footwear.

5. Author's Contribution

- **Conceptualization** – Alexandre Oka Thomaz Cordeiro; Cristiane Reis Martins.
- **Data curation** – Alexandre Oka Thomaz Cordeiro; Cristiane Reis Martins.
- **Formal analysis** – Alexandre Oka Thomaz Cordeiro; Cristiane Reis Martins.
- **Funding acquisition** – Cristiane Reis Martins.
- **Investigation** – Alexandre Oka Thomaz Cordeiro; Cristiane Reis Martins.
- **Methodology** – Alexandre Oka Thomaz Cordeiro; Marcelo Eduardo da Silva; Cristiane Reis Martins.
- **Project administration** – Cristiane Reis Martins.
- **Resources** – Cristiane Reis Martins.
- **Software** – NA.
- **Supervision** – Cristiane Reis Martins.
- **Validation** – Alexandre Oka Thomaz Cordeiro; Cristiane Reis Martins.
- **Visualization** – Alexandre Oka Thomaz Cordeiro; Cristiane Reis Martins.
- **Writing** – original draft – Alexandre Oka Thomaz Cordeiro; Cristiane Reis Martins.
- **Writing** – review & editing – Alexandre Oka Thomaz Cordeiro; Marcelo Eduardo da Silva; Cristiane Reis Martins.

6. Acknowledgments

The authors thank Alpargatas S.A., Hamilton Rios Ind. Com. e Exp., Flexlab Consultoria e Treinamento Ltda, and Centro de Equipamentos e Serviços Multiusuários (CESM-ICAQF) at UNIFESP, Diadema Campus.

7. References

1. Abreu, C. S., & Silva, A. P. (2024). Improving the circular economy in the footwear industry. *European Journal of Materials Science and Engineering*, 9(3), 175-182. <http://doi.org/10.36868/ejmse.2024.09.03.175>.
2. Elayaraja, K., & Kumar, M. V. (2024). Innovations in non-leather footwear design and development. *International Journal of Research Publication and Reviews*, 5(6), 5975-5978. Retrieved in 2025, February 26, from <https://ijrpr.com/uploads/V5ISSUE6/IJRPR30510.pdf>
3. Specht, I. R., Froehlich, C., Bondan, J., & Nodari, C. H. (2024). Frugal innovation and sustainability in the footwear sector. *Revista de Administração Contemporânea*, 28(3), e230228. <http://doi.org/10.1590/1982-7849rac2024230228>.
4. Asabuwa Ngwabebhoh, F., Saha, N., Saha, T., & Saha, P. (2022). Bio-innovation of new-generation nonwoven natural fibrous materials for the footwear industry: current state-of-the-art and sustainability panorama. *Journal of Natural Fibers*, 19(13), 4897-4907. <http://doi.org/10.1080/15440478.2020.1870635>.

5. Munny, A. A., Ali, S. M., Kabir, G., Moktadir, M. A., Rahman, T., & Mahtab, Z. (2019). Enablers of social sustainability in the supply chain: an example of footwear industry from an emerging economy. *Sustainable Production and Consumption*, 20, 230-242. <http://doi.org/10.1016/j.spc.2019.07.003>.
6. Conti, T. M., Catto, A. L., & Amico, S. C. (2022). Composite for insole shoe assembly based on polyvinyl acetate and polyester fabric waste from the footwear industry. *Polymer Composites*, 43(10), 7360-7371. <http://doi.org/10.1002/pc.26813>.
7. Ferreira, C. A., Serrano, C. L. R., & Kuyven, P. S. (2011). Use of analysis of variance and linear regression as a prediction tool for mechanical performance of SBR. *Plastics, Rubber and Composites*, 40(1), 40-45. <http://doi.org/10.1179/174328911X12940139029329>.
8. Pikoń, K., Poranek, N., Marczak, M., Łaźniewska-Piekarczyk, B., & Ściński, W. (2024). Raw and pre-treated styrene butadiene rubber (SBR) dust as a partial replacement for natural sand in mortars. *Materials (Basel)*, 17(2), 441. <http://doi.org/10.3390/ma17020441>. PMID:38255609.
9. Van Rensburg, M. L., Nkomo, S. L., & Mkhize, N. M. (2020). Life cycle and end-of-life management options in the footwear industry: a review. *Waste Management & Research*, 38(6), 599-613. <http://doi.org/10.1177/0734242X20908938>. PMID:32181706.
10. Bashpa, P., Bijudas, K., Dileep, P., Elanthikkal, S., & Francis, T. (2022). Reutilization of polyurethane-based shoe sole scrap as a reinforcing filler in natural rubber for the development of high-performance composites. *Journal of Elastomers and Plastics*, 54(6), 1040-1060. <http://doi.org/10.1177/00952443221108514>.
11. Alves, L. M. F., Luna, C. B. B., Costa, A. R. M., Ferreira, E. S. B., Nascimento, E. P., & Araújo, E. M. (2024). Toward the reuse of styrene-butadiene (SBRr) waste from the shoes industry: Production and compatibilization of BioPE/SBRr blends. *Polymer Bulletin*, 87(11), 10311-10336. <http://doi.org/10.1007/s00289-024-05181-5>.
12. Marsura, G., Bahú, J. O., Tovar, L. P., Fernandez-Felisbino, R., & Gomes, E. L. (2024). Recycled PVC to eco-friendly materials for footwear industry: process and mechanical properties. *Polímeros: Ciência e Tecnologia*, 34(4), e20240040. <http://doi.org/10.1590/0104-1428.20240064>.
13. Pereira, D. C., Farias, L. A., Perazzo, B. N., & Torres, M. S. (2014). Light cementitious composites with wastes from the footwear industry. *Key Engineering Materials*, 600, 648-656. <http://doi.org/10.4028/www.scientific.net/KEM.600.648>.
14. Sobrinho, E. D. M., Ferreira, E. S. B., Silva, F. U., Bezerra, E. B., Wellen, R. M. R., Araújo, E. M., & Luna, C. B. B. (2024). From waste to Styrene-Butadiene (SBR) reuse: developing PP/SBR/SEP mixtures with carbon nanotubes for antistatic application. *Polymers*, 16(17), 2542. <http://doi.org/10.3390/polym16172542>. PMID:39274174.
15. Kohan, L., Martins, C. R., Duarte, L. O., Pinheiro, L., & Barúque-Ramos, J. (2019). Panorama of natural fibers applied in Brazilian footwear: materials and market. *SN Applied Sciences*, 1(8), 895. <http://doi.org/10.1007/s42452-019-0927-0>.
16. Lozada, E. R., Aguilar, C. M. G., Carvalho, J. A. J., Sánchez, J. C., & Torres, G. B. (2023). Vegetable cellulose fibers in natural rubber composites. *Polymers*, 15(13), 2914. <http://doi.org/10.3390/polym15132914>. PMID:37447558.
17. Pereira, P. H. F., Rosa, M. F., Cioffi, M. O. H., Benini, K. C. C., Milanese, A. C., Voorwald, H. J. C., & Mulinari, D. R. (2015). Vegetal fibers in polymeric composites: a review. *Polímeros: Ciência e Tecnologia*, 25(1), 9-22. <http://doi.org/10.1590/0104-1428.1722>.
18. Prashanth, S., Subbaya, K. M., Nithin, K., & Sachhidananda, S. (2017). Fiber reinforced composites – A review. *Journal of Marine Science and Engineering*, 6(3), 341. <http://doi.org/10.4172/2169-0022.1000341>.
19. Lopes, F. F. M., Araújo, G. T., Nascimento, J. W. B., Gadelha, T. S., & Silva, V. R. (2010). Estudo dos efeitos da acetilação em fibras de sisal. *Revista Brasileira de Engenharia Agrícola e Ambiental*, 14(7), 783-788. <http://doi.org/10.1590/S1415-43662010000700015>.
20. Pappu, A., Saxena, M., Thakur, V. K., Sharma, A., & Haque, R. (2016). Facile extraction, processing, and characterization of biorenewable sisal fibers for multifunctional applications. *Journal of Macromolecular Science, Part A: Pure and Applied Chemistry*, 53(7), 424-432. <http://doi.org/10.1080/10601325.2016.1176443>.
21. Jacob, M., Thomas, S., & Varughese, K. T. (2006). Novel woven sisal fabric reinforced natural rubber composites: tensile and swelling characteristics. *Journal of Composite Materials*, 40(16), 1471-1485. <http://doi.org/10.1177/0021998306059731>.
22. Iozzi, M. A., Martins, G. S., Martins, M. A., Ferreira, F. C., Job, A. E., & Mattoso, L. H. C. (2010). Estudo da influência de tratamentos químicos da fibra de sisal nas propriedades de compósitos com borracha nitrílica. *Polímeros: Ciência e Tecnologia*, 20(1), 25-32. <http://doi.org/10.1590/S0104-14282010005000003>.
23. Martin, A. R., Martins, M. A., Mattoso, L. H. C., & Silva, O. R. R. F. (2009). Caracterização química e estrutural de fibra de sisal da variedade Agave sisalana. *Polímeros: Ciência e Tecnologia*, 19(1), 40-46. <http://doi.org/10.1590/S0104-14282009000100011>.
24. Prasantha Kumar, R., Manikandan Nair, K. C., Thomas, S., Schit, S. C., & Ramamurthy, K. (2000). Morphology and melt rheological behaviour of short-sisal-fibre-reinforced SBR composites. *Composites Science and Technology*, 60(9), 1737-1751. [http://doi.org/10.1016/S0266-3538\(00\)00057-9](http://doi.org/10.1016/S0266-3538(00)00057-9).
25. Li, Y., Mai, Y.-W., & Ye, L. (2000). Sisal fiber and its composites: A review of recent developments. *Composites Science and Technology*, 60(11), 2037-2055. [http://doi.org/10.1016/S0266-3538\(00\)00101-9](http://doi.org/10.1016/S0266-3538(00)00101-9).
26. John, M. J., & Anandjiwala, R. D. (2008). Recent developments in chemical modification and characterization of natural fiber-reinforced composites. *Polymer Composites*, 29(2), 187-207. <http://doi.org/10.1002/pc.20461>.
27. Roy, K., Debnath, S. C., Pongwisuthiruchte, A., & Potiyaraj, P. (2021). Recent advances of natural fibers based green rubber composites: properties, current status, and future perspectives. *Journal of Applied Polymer Science*, 138(35), 50866. <http://doi.org/10.1002/app.50866>.
28. Chandrasekar, M., Ishak, M. R., Sapuan, S. M., Leman, Z., & Jawaid, M. (2017). A review on the characterisation of natural fibres and their composites after alkali treatment and water absorption. *Plastics, Rubber and Composites*, 46(3), 119-136. <http://doi.org/10.1080/14658011.2017.1298550>.
29. Ma, L., He, H., Jiang, C., Zhou, L., Luo, Y., & Jia, D. (2012). Effect of alkali treatment on structure and mechanical properties of acrylonitrile-butadiene-styrene/bamboo fiber composites. *Journal of Macromolecular Science, Part B: Physics*, 51(11), 2232-2244. <http://doi.org/10.1080/00222348.2012.669688>.
30. Li, X., Tabil, L. G., & Panigrahi, S. (2007). Chemical treatments of natural fiber for use in natural fiber-reinforced composites: a review. *Journal of Polymers and the Environment*, 15(1), 25-33. <http://doi.org/10.1007/s10924-006-0042-3>.
31. Mani, P., & Satyanarayana, K. G. (1990). Effects of the surface treatments of lignocellulosic fibers on their debonding stress. *Journal of Adhesion Science and Technology*, 4(1), 17-24. <http://doi.org/10.1163/156856190X00036>.
32. Srisuwan, S., Prasertsopha, N., Suppakarn, N., & Chumsamrong, P. (2014). The effects of alkalinized and silanized woven sisal fibers on mechanical properties of natural rubber modified epoxy resin. *Energy Procedia*, 56, 19-25. <http://doi.org/10.1016/j.egypro.2014.07.127>.

33. Iozzi, M. A., Martins, M. A., & Mattoso, L. H. C. (2004). Propriedades de compósitos híbridos de borracha nitrílica, fibras de sisal e carbonato de cálcio. *Polímeros: Ciência e Tecnologia*, 14(2), 93-98. <http://doi.org/10.1590/S0104-14282004000200012>.
34. Lima, P. R. L., Santos, R. J., Ferreira, S. R., & Toledo, R. D., Fo. (2013). Characterization and treatment of sisal fiber residues for cement-based composite application. *Engenharia Agrícola*, 34(5), 812-825. <http://doi.org/10.1590/S0100-69162014000500002>.
35. Xie, Y., Hill, C. A. S., Xiao, Z., Militz, H., & Mai, C. (2010). Silane coupling agents used for natural fiber/polymer composites: a review. *Composites. Part A, Applied Science and Manufacturing*, 41(7), 806-819. <http://doi.org/10.1016/j.compositesa.2010.03.005>.
36. Rong, M. Z., Zhang, M. Q., Liu, Y., Yang, G. C., & Zeng, H. M. (2001). The effect of fiber treatment on the mechanical properties of unidirectional sisal-reinforced epoxy composites. *Composites Science and Technology*, 61(10), 1437-1447. [http://doi.org/10.1016/S0266-3538\(01\)00046-X](http://doi.org/10.1016/S0266-3538(01)00046-X).
37. Sreekumar, P. A., Saiah, R., Saiter, J. M., Leblanc, N., Joseph, K., Unnikrishnan, G., & Thomas, S. (2008). Thermal behavior of chemically treated and untreated sisal fiber reinforced composites fabricated by resin transfer molding. *Composite Interfaces*, 15(6), 629-650. <http://doi.org/10.1163/156855408785971317>.
38. Bledzki, A. K., & Gassan, J. (1999). Composites reinforced with cellulose based fibres. *Progress in Polymer Science*, 24(2), 221-274. [http://doi.org/10.1016/S0079-6700\(98\)00018-5](http://doi.org/10.1016/S0079-6700(98)00018-5).
39. Rajkumar, S., Tjong, J., Nayak, S. K., & Sain, M. (2015). Wetting behavior of soy-based resin and unsaturated polyester on surface-modified sisal fiber mat. *Journal of Reinforced Plastics and Composites*, 34(10), 807-818. <http://doi.org/10.1177/0731684415580630>.
40. Bledzki, A. K., Reihmane, S., & Gassan, J. (1996). Properties and modification methods for vegetable fibers for natural fiber composites. *Journal of Applied Polymer Science*, 59(8), 1329-1336. [http://doi.org/10.1002/\(SICI\)1097-4628\(19960222\)59:8<1329::AID-APP17>3.0.CO;2-0](http://doi.org/10.1002/(SICI)1097-4628(19960222)59:8<1329::AID-APP17>3.0.CO;2-0).
41. Satyanarayana, K. G., Sukumaran, K., Mukherjee, P. S., Pavithran, C., & Piuai, S. G. K. (1990). Natural fibre-polymer composites. *Cement and Concrete Composites*, 12(2), 117-136. [http://doi.org/10.1016/0958-9465\(90\)90049-4](http://doi.org/10.1016/0958-9465(90)90049-4).
42. Abdelsalam, A. A., Araby, S., El-Sabbagh, S. H., Abdelmoneim, A., & Hassan, M. A. (2021). A comparative study on mechanical and rheological properties of ternary rubber blends. *Polymers & Polymer Composites*, 29(1), 15-28. <http://doi.org/10.1177/0967391119897177>.
43. Charoeythornkhajhornchai, P., Samthong, C., Boonkerd, K., & Somwangthanaroj, A. (2017). Effect of azodicarbonamide on microstructure, cure kinetics and physical properties of natural rubber foam. *Journal of Cellular Plastics*, 53(3), 287-303. <http://doi.org/10.1177/0021955X16652101>.
44. Haghighat, M., Zadhoush, A., & Nouri Khorasani, S. (2005). Physicomechanical properties of α -cellulose-filled styrene-butadiene rubber composites. *Journal of Applied Polymer Science*, 96(6), 2203-2211. <http://doi.org/10.1002/app.21691>.
45. Meissner, N., & Rzymiski, W. M. (2013). Use of short fibers as a filler in rubber compounds. *AUTEX Research Journal*, 13(2), 40-43. <http://doi.org/10.2478/v10304-012-0025-5>.
46. Bosselmann, S., Frank, T., Wieltzka, M., & Ortmaier, T. (2018). *Optimization of process parameters for rubber curing in relation to vulcanization requirements and energy consumption*. In *Proceedings of the 2018 IEEE/ASME International Conference on Advanced Intelligent Mechatronics (AIM)* (pp. 804-809). USA: IEEE. <http://doi.org/10.1109/AIM.2018.8452354>.
47. Martins, M. A., & Mattoso, L. H. C. (2004). Short sisal fiber-reinforced tire rubber composites: dynamic and mechanical properties. *Journal of Applied Polymer Science*, 91(1), 670-677. <http://doi.org/10.1002/app.13210>.
48. Papagiannis, P., Koutkalaki, Z., Azariadis, P., & Papanikos, P. (2016). Definition and evaluation of plantar mechanical comfort for the support of footwear design. *Computer-Aided Design and Applications*, 13(2), 162-172. <http://doi.org/10.1080/16864360.2015.1084189>.
49. Buitrago, O., Palacio, O., & Delgado, E. (2017). Evaluation of silanes in SBR 1502/Telinne monspessulana flour composites. *Polímeros: Ciência e Tecnologia*, 27(2), 116-121. <http://doi.org/10.1590/0104-1428.2206>.
50. Changjie, Y., Zhang, Q., Junwei, G., Junping, Z., Youqiang, S., & Yuhang, W. (2011). Cure characteristics and mechanical properties of styrene-butadiene rubber/hydrogenated acrylonitrile-butadiene rubber/silica composites. *Journal of Polymer Research*, 18(6), 2487-2494. <http://doi.org/10.1007/s10965-011-9670-y>.

Received: Feb. 26, 2025

Revised: May 07, 2025

Accepted: May 30, 2025

Associate Editor: Artur J. M. Valente